ELSEVIER

Biophysical Chemistry 128 (2007) 30–37

Biophysical Chemistry

http://www.elsevier.com/locate/biophyschem

Electrochemical behavior of caffeic acid at single-walled carbon nanotube:graphite-based electrode

Abdolmajid Bayandori Moghaddam [a], Mohammad Reza Ganjali [a,*], Rassoul Dinarvand [b], Parviz Norouzi [a], Ali Akbar Saboury [c], Ali Akbar Moosavi-Movahedi [c]

[a] Center of Excellence in Electrochemistry, Faculty of Chemistry, University of Tehran, P. O. Box: 14155-6455, Tehran, Iran
[b] Medical Nanotechnology Research Centre, Tehran University of Medical Sciences, Tehran, P.O. Box 14155-6451, Iran
[c] Institute of Biochemistry and Biophysics, University of Tehran, Tehran, Iran

Received 14 February 2007; received in revised form 28 February 2007; accepted 28 February 2007
Available online 7 March 2007

Abstract

The performance of a single-walled carbon nanotube:graphite-based electrode, prepared by mixing single-walled carbon nanotubes (SWCNTs) and graphite powder, is described. The resulting electrode shows an excellent behavior for the redox of caffeic acid (CA), an important biological molecule. Due to the existing resemblance between electrochemical and biological reactions, it can be assumed that the oxidation mechanisms on the electrode and in the body share similar principles. SWCNT:graphite-based electrode presents a significant decrease in the overvoltage for the CA oxidation as well as a dramatic improvement in the reversibility of the CA redox behavior in comparison with the graphite-based and glassy carbon (GC) electrodes.

Keywords: Carbon nanotube; Caffeic acid; Electrochemical properties; Modified electrode

1. Introduction

The rapid progress in nanotechnology and nanoscience introduces a scientific momentum that involves the fundamental comprehension of the nanostructure properties, the synthesis and plans in nanoscale. Carbon and, particularly, graphite in its various forms, is an attractive electrode material. Two areas of special interest are the modified carbon electrodes and the carbon nanotube electrodes. In 1991, Iijima discovered microtubules of graphitic carbon with outer diameters of 4–30 nm and a length of up to 1 μm, naming these tubes multiwalled carbon nanotubes (MWCNTs) [1]. In addition, a report of carbon fibers down to 4 nm in diameter, found on a carbon arc electrode, was published by Wiles and co-workers [2,3]. Single-walled carbon nanotubes (SWCNTs), which are seamless cylinders each made of a single graphene sheet, were first reported in 1993 [4,5]. The unique structures lead to unique SWCNTs properties, mechanical strength greater than that of Fe, density lower than that of Al and thermal stability at 1400 °C in a vacuum. Furthermore, they illustrate wide potential window, chemical inertness, low cost and suitability for various sensing and defection. Depending on their atomic structure, CNTs behave electrically as a metal or as a semiconductor [6,7]. The subtle electronic properties suggest that CNTs have the ability to promote electron-transfer reactions, when used as an electrode in chemical reactions [8,9]. Recent studies demonstrated that a CNT modified electrode could impart strong electrocatalytic activity to some important biomolecules [9–11].

Many biological activities have been reported for free caffeic acid (CA) [12–19]. In several plant species, the levels of caffeic acid and other phenolics appear to be related to pest resistance [20–22]. Caffeic acid is one of the many phenolics considered to be an important part of the general plant defense mechanism against infection predation [23,24]. Caffeic acid esters, such as caffeic acid phenethyl (CAPE) and benzyl esters, display selective antiproliferative activity against some types of cancer cells [25].

Moreover, the electrochemical method is rapid and inexpensive for the study of this important category of molecules and biologically important molecules [26–31] and due to the

* Corresponding author. Tel.: +98 21 61112294; fax: +98 21 66405141.
E-mail address: Ganjali@khayam.ut.ac.ir (M.R. Ganjali).

0301-4622/$ - see front matter © 2007 Elsevier B.V. All rights reserved.
doi:10.1016/j.bpc.2007.02.006

existing resemblance between electrochemical and biological reactions, it can be assumed that the oxidation mechanisms on the electrode and in the body share similar principles [32]. In this paper, the CA electrochemical behavior at a SWCNT:graphite-based electrode was studied by cyclic voltammetry (CV).

2. Experimental details

2.1. Chemical reagents

The caffeic acid (3,4-dihydroxy cinnamic acid), the graphite powder, acids and the used salts for the preparation of buffer solutions (c=0.15 M) were reagent grade materials from Merck and were used without any further purification. The single-walled carbon nanotubes (SWCNTs) were purchased from Research Institute of the Petroleum Industry (Iran). All solutions were prepared with deionized water.

2.2. Measurements

All electrochemical experiments were performed by the Autolab potentiostat PGSTAT 30 (Eco Chemie B.V., Netherlands), equipped with the GPES 4.9 software. A three-electrode cell was also used, employing a glassy-carbon (GC), graphite and SWCNT:graphite based composite, acting as the working electrodes. A platinum wire was applied as the counter electrode and Ag|AgCl|KCl (sat.) was applied as the reference electrode. All potentials were reported with respect to this reference. All experiments were carried out at 25±1 °C.

Furthermore, the scanning electron microscope (SEM) images were recorded using a ZEISS DSM 960, while the transmission electron microscope (TEM) studies were performed with the help of a Phillips transmission electron microscope.

Gaussian 98, Revision A. 6, program has been used for the quantum mechanic calculations. The B3LYP/6–31G* method is employed for the gas-phase molecular geometry and HF/6–31G* method is used for the obtained atomic charges (ESP fit) (Fig. 1) [33].

2.3. Preparation of the SWCNT:graphite-based electrode

For the electrochemical studies, the SWCNT:graphite-based electrodes were prepared from a mixture of SWCNTs and graphite powder in the ratio of 1:1 (w/w). Regarding the casting procedure, a small amount of melted paraffin (~20% by weight) was added to the SWCNT:graphite powder mixture. A portion of the composite mixture was packed into the end of a polyamide tube. The electrical contact was made by forcing a glassy carbon rod (r=1.5 mm) down into the tube and into the back of the composite and, then, a thin film on the surface of the glassy carbon electrode. This strategy increased the compactness and stability of the composite on the surface of the glassy carbon electrode. Here, it should be mentioned that only a very small amount of melted paraffin had to be used for the attachment of composite, because in this way a hard composite creation was achieved, illustrating excellent electrochemical properties. In addition, the employment of a greater melted paraffin amount raised the peak potentials. Pure SWCNT or graphite-based electrodes were also made using the separate materials, dispersed in a small quantity of melted paraffin, in the same way as for the composite electrodes described above. The GC rod was carefully polished with alumina (0.05 μm) by a polishing cloth. The electrode was placed in ethanol and sonicated to remove the adsorbed particles.

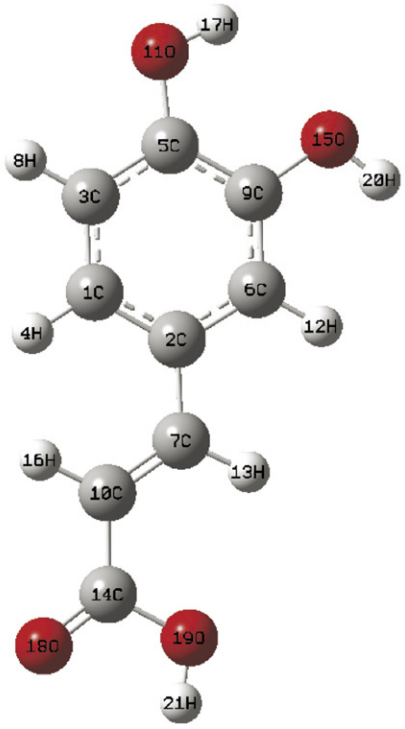

Fig. 1. Optimized geometry (B3LYP/6–31G*) of CA.

3. Results and discussions

3.1. TEM characterization

Fig. 2 shows the structure of the SWCNTs pipe clearly. Fig. 2 (a and b) illustrate the scanning electron microscope (SEM) image and Fig. 2c presents the transmission electron microscope (TEM) image of the SWCNTs structure. Some SWCNTs were formed as boundless tubes because of the van der Waals forces.

3.2. Electrochemical behavior of CA at the SWCNT: graphite-based electrode

Fig. 3a and b show the cyclic voltammograms of 0.06 mM caffeic acid (CA) on the surface of the SWCNT-based and SWCNT:graphite-based (2:1) electrodes. The pure SWCNT-based electrode or the electrode with the greater SWCNT ratio did not exhibit excellent electrochemical behavior for the CA, on the grounds that the attachment and compactness of the SWCNT: graphite composite decreased with the SWCNT increase. However, this phenomenon increased with the increasing of the graphite ratio in the composite. The best electrochemical behavior was obtained on the SWCNT:graphite surface with the ratio of

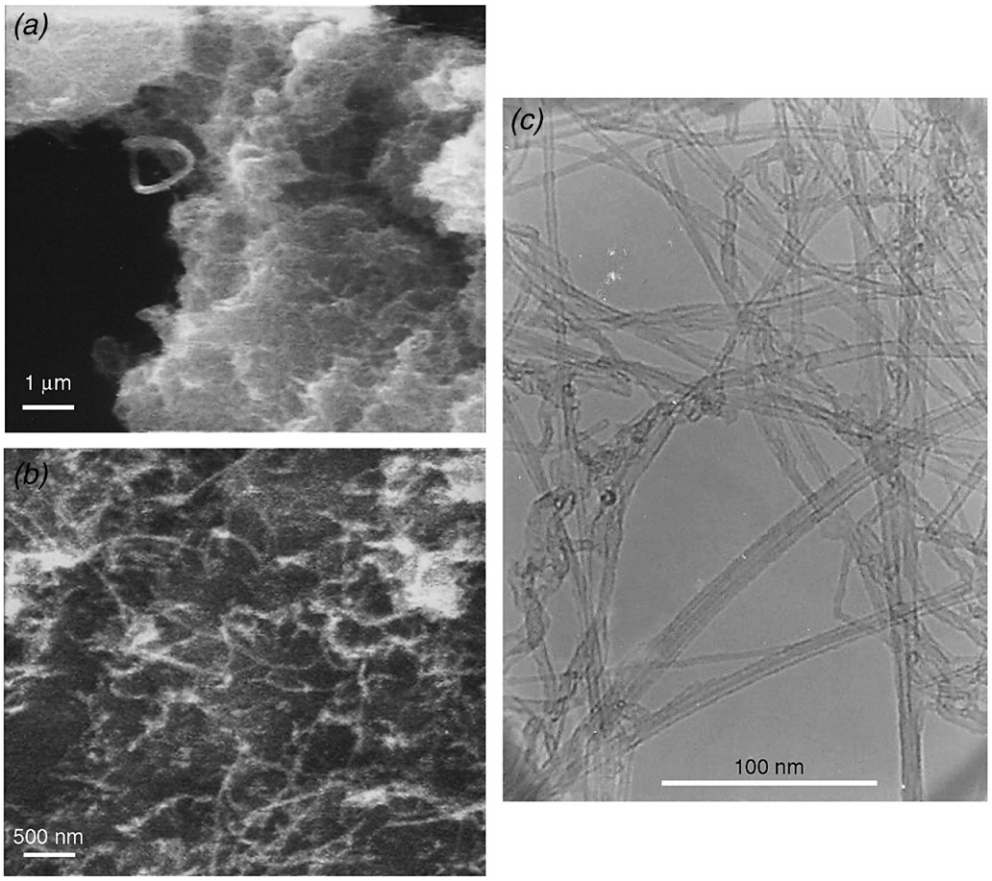

Fig. 2. SEM (a and b) and TEM (c) images of the single-walled carbon nanotubes.

1:1, named earlier as SWCNT:graphite-based electrode. Fig. 3c–e depict comparative cyclic voltammograms (CVs) obtained at the SWCNT:graphite-based electrode (c), graphite-based electrode (d) and GC electrode (e), after the addition of 0.06 mM CA in phosphate buffer solution (PBS, pH=7.0). The presence of well-defined reversible anodic and cathodic peaks indicated improved

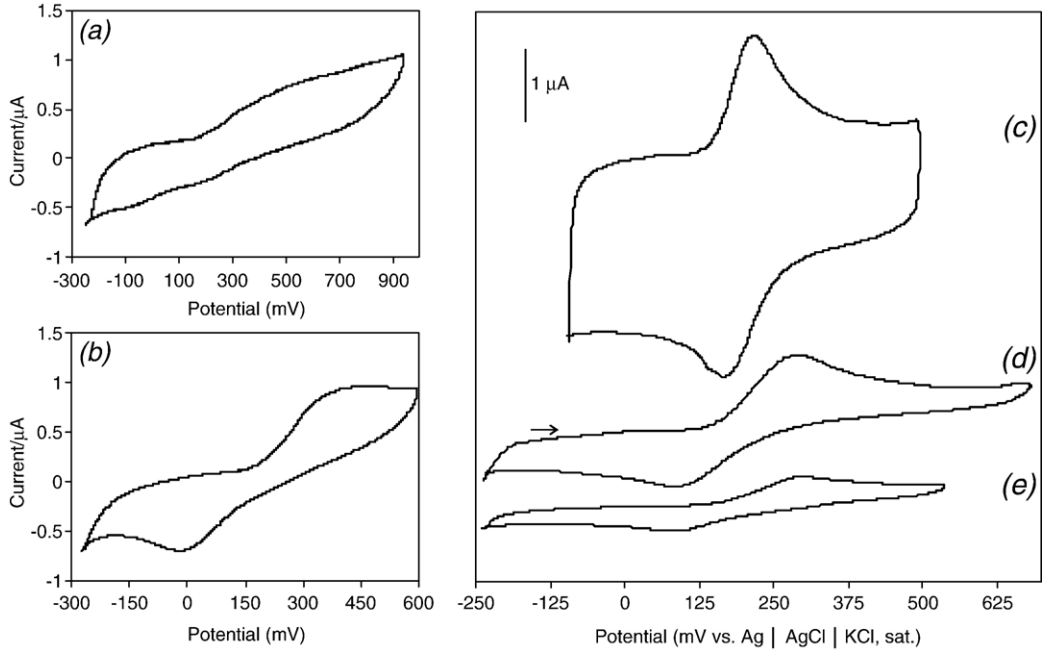

Fig. 3. Comparative cyclic voltammograms of 0.06 mM CA on the surface of (a) SWCNT-based electrode, (b) SWCNT:graphite-based electrode (2:1), (c) SWCNT: graphite-based electrode, (d) graphite-based electrode and (e) GC electrode in PBS (pH=7.0). Scan rate: 50 mV s^{-1}. The arrow indicates the initial scan direction.

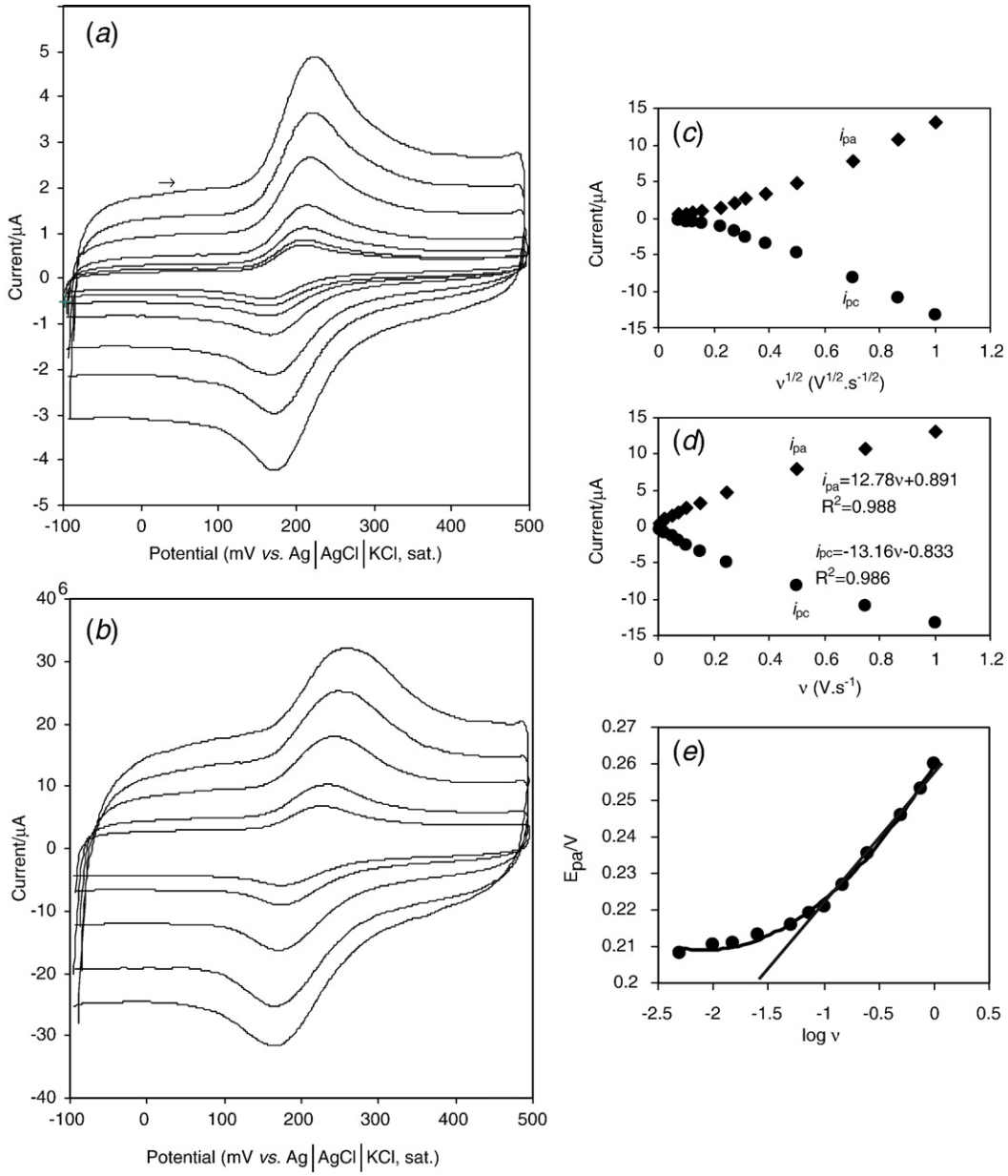

Fig. 4. (a and b) Cyclic voltammograms of CA on SWCNT:graphite-based electrode in PBS (pH = 7.0) at various sweep rates. The arrows are indicating the direction of the decreasing sweep rate: 1, 0.75, 0.50, 0.25, 0.15, 0.10, 0.075, 0.050, 0.025, 0.015, 0.010 and 0.005 V s^{-1}. The relationship between the peak currents (i_{pa}, i_{pc}) *vs.* the square root of sweep rates (c) and the sweep rates (d). (e) Dependence of anodic peak potential on log *v*.

electrochemical reactivity for the CA oxidation–reduction reaction on the SWCNT:graphite-based electrode (Fig. 3c). The CVs present a characteristic anodic peak at E_{pa} = 0.297 V for the GC electrode, at E_{pa} = 0.291 V for the graphite-based electrode and at E_{pa} = 0.218 V *vs.* Ag|AgCl|KCl, sat. for the SWCNT: graphite-based electrode. The complementary cathodic peak

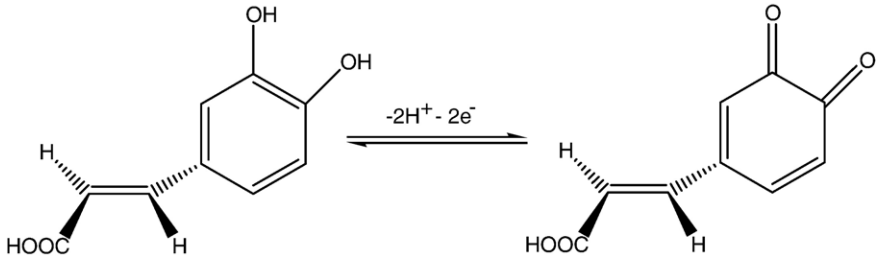

Fig. 5. Redox mechanism of CA.

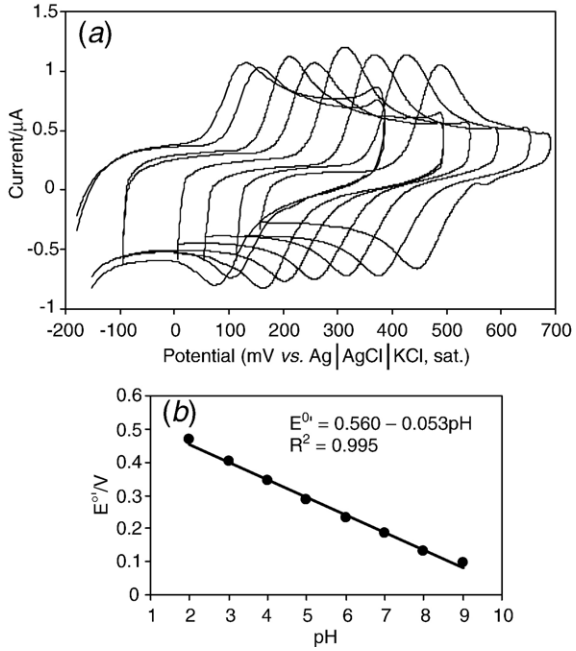

Fig. 6. (a) Cyclic voltammograms of 0.06 mM CA on the surface of the SWCNT:graphite-based electrode at various pH values (c=0.15 M) from positive potentials to negative potentials with pH=2, 3, 4, 5, 6, 7, 8 and 9, respectively. Scan rate: 15 mV s^{-1}. (b) The relationship between the formal potential and pH values.

appeared at E_{pc}=0.84 V for GC, at 0.81 V for graphite and at 0.166 V for the SWCNT:graphite-based electrode. The difference between E_{pa} and E_{pc} (ΔE_p) decreased from 0.213 V for the GC electrode, 0.210 V for the graphite-based electrode to 0.052 V for the SWCNT:graphite-based electrode. Thus, the CA reversibility was significantly improved. The reason for the better performance of the SWCNT:graphite-based electrode might be due to the nanometer dimensions of the SWCNTs, the electronic structure and the topological defects present on the SWCNTs surfaces [34]. The SWCNTs augmented the effective area of the electrode. The SWCNT:graphite-based electrode presents no electrochemical activity in the used solutions, but the background current became larger. To further investigate the characteristics of CA at the SWCNT:graphite-based electrode, the influence of the scan rate on the oxidation of CA was studied by cyclic voltammetry (Fig. 4a–d). With the scan rate increase, the peak current raised. The peak current of CA increased linearly with the scan rate (v) in the range from 0.005 to 1.0 V s^{-1} (Fig. 4d). This means that the electrode process is controlled by adsorption. On the other hand, with the increase of the scan rates, the oxidation peaks shifted to more positive potentials, while the reduction peaks shifted to more negative potentials with smaller potential shifted in comparison with the oxidation potential shifts, indicating that the electron-transfer rate was not very fast and the electrochemical reaction gradually became less reversible. As shown in Fig. 4e, at higher scan rates, the anodic peak potentials *vs.* log v show a linear relationship. The regression equation is E_{pa}=0.0355 log v+ 0.2581 (R^2=0.996, E_p: V, v: V s^{-1}). According to the equation [35]: $E_{0a}=E^{0\prime}+m$ [0.78+ln ($D^{1/2}$ k_s^{-1})−0.5 ln m]+(m/2) ln v ($m=RT/[(1-\alpha)n_\alpha F]$, the electron transfer coefficient α is estimated to be 0.57 at SWCNT:graphite-based electrode. The electrochemical behavior of CA is irreversible at the GC

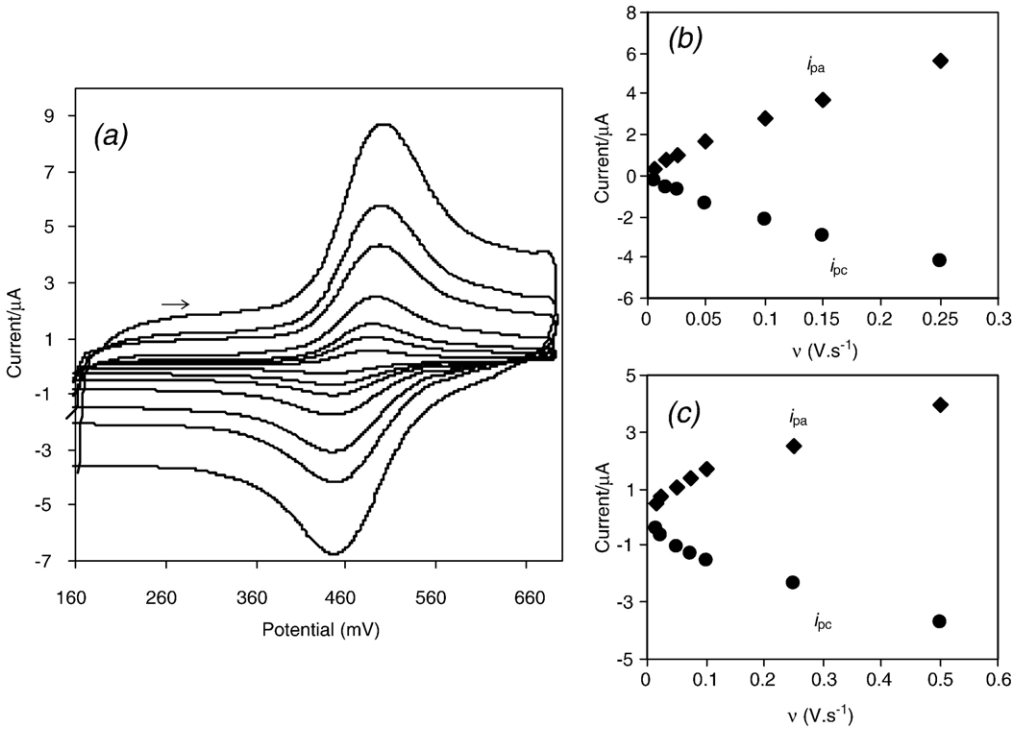

Fig. 7. (a) Cyclic voltammograms of CA in sulphate buffer (pH=2.0) at various sweep rates. The arrows are indicating the direction of the decreasing sweep rate: 0.25, 0.15, 0.10, 0.05, 0.025, 0.015, and 0.005 V s^{-1}, other conditions as in Fig. 4. (b) The relationship between the peak currents (i_{pa}, i_{pc}) *vs.* the sweep rates, (c) as (b) in carbonate buffer pH=9.0 at 0.50, 0.25, 0.10, 0.075, 0.050, 0.025 and 0.015 V s^{-1}.

electrode. The peak potential, E_p is a function of the scan rate [36]. The electron transfer coefficient α is found to be 0.86 at the GC electrode.

From the CV of CA at the SWCNT:graphite-based electrode (Fig. 3c), at the E_{pa} value of 0.218 V and at the $E_{pa/2}$ value of 0.186 V, a reversible system was obtained [36].

$$|E_p - E_{p/2}| = \frac{56.5}{n}\text{mV}. \quad (1)$$

The charge transfer number (n) was also calculated to be approximately 2. As CA redox behavior involved the transfer of two protons (Fig. 5), we analyzed the pH effect on the cyclic voltammogram at the SWCNT:graphite-based electrode. Fig. 6a demonstrates the CVs of 0.06 mM CA in different buffer solutions (c=0.15 M) with various pH values, ranging from 2.0 to 9.0. The cathodic and anodic peak potentials shifted to more negative values. Fig. 6d displays the average variation of the anodic and cathodic peak potentials for the CA oxidation with pH at the SWCNT:graphite-based electrode. This average could be considered approximately as the standard (formal) potential ($E°'$). At the SWCNT:graphite-based electrode, with the increase of the solution pH, the formal potential (and the cathodic and the anodic peak potentials) decreased by about 56 mV per pH unit, corresponding to a two-electron–two-proton overall redox process and obeyed the following equation [37]:

$$E°' = E° - 2.303(mRT/nF)\text{pH} \quad (2)$$

Here, m and n are the proton and electron numbers in the redox reaction, respectively. R is the gas constant and T is the absolute temperature. Based on the relation between $E°'$ and pH, the standard formal potential $E°$ was obtained from the intercept of Fig. 6b ($E°$=0.560 V). The proton number (m), intervening in the redox process, was approximately 2, which could be calculated from the slope of the equation above. Therefore, the proposed redox mechanism for CA could be written as depicted in Fig. 5.

Fig. 7 illustrates the CVs of CA in pH=2.0. According to Fig. 7b and c, there is a good linear relationship between the peak current and the scan rate (v) at pH=2.0 (Fig. 7b) and pH=9.0 (Fig. 7c). This means that the electrode process is controlled by adsorption in both acidic and basic solutions.

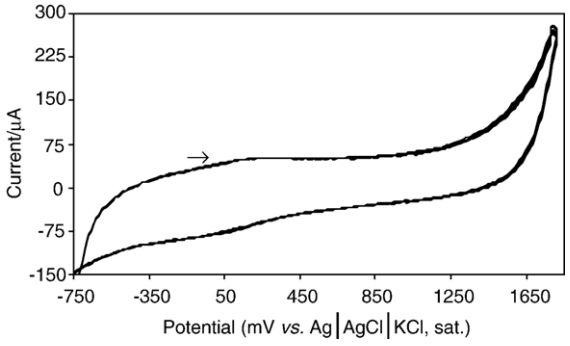

Fig. 8. Electrochemical behavior of the SWCNT-based electrode in the acetate buffer (pH=4.0) during the continuous cyclic voltammograms.

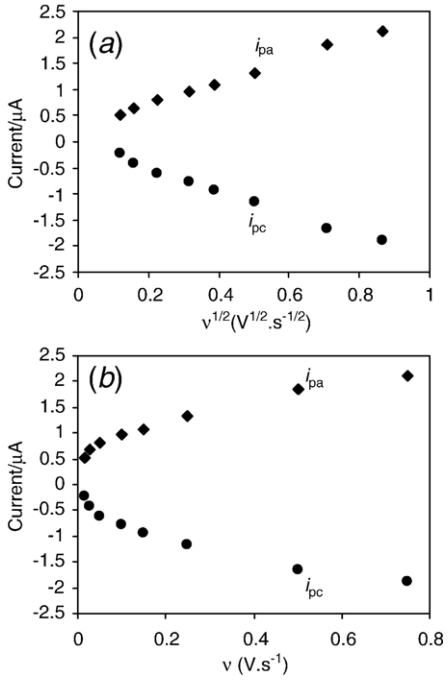

Fig. 9. The relationship between the peak currents (i_{pa}, i_{pc}) *vs.* the square root of the sweep rates (a) and sweep rates (b) for 0.06 mM CA at the graphite-based electrode in PBS (pH=7.0) at 0.75, 0.50, 0.25, 0.15, 0.10, 0.05, 0.025 and 0.015 V s^{-1}.

Fig. 8 demonstrates CVs of the SWCNT-based electrode in the absence of any oxidation or reduction process. This is, indeed, an advantage for the SWCNT substrates, as they are sufficiently stable in an extensive potential region. Oxidation or reduction of the substrate surface may lead to unfavorable process.

The influence of the scan rate on the CA oxidation at the graphite-based electrode was studied by cyclic voltammetry. Fig. 9 depicts the anodic and cathodic peak currents of CA at the graphite-based electrode at pH=7.0 at various scan rates. According to Fig. 9a, the redox peak currents of CA increased linearly with the square root of the scan rate. This means that the CA electrochemical behavior at the graphite-based electrode was a diffusion-controlled process.

3.3. Theoretical characteristics of caffeic acid

On the one hand, the electrode process was controlled by adsorption on the surface of the SWCNT:graphite-based electrode (Fig. 4) and it was controlled by diffusion on the surface of the graphite-based electrode (Fig. 9). On the other hand, during the CA electro-oxidation, positive potentials were applied to the electrode. Therefore, the CA atoms with the more negative charges could be the adsorbed sites of CA on the SWCNTs surfaces. For this reason, the calculation of the CA atomic charges might be very useful. The CA atomic charges are presented in Fig. 10. According to the CA atomic charge, the higher negative charges are related to the oxygen atoms and the highest negative charge among the oxygen atoms is attributed to the oxygen atom of the hydroxyl group in carboxylic acid group. In detail, the oxygen atom of the hydroxyl in carboxylic acid group presents the highest negative charge (−0.687), in

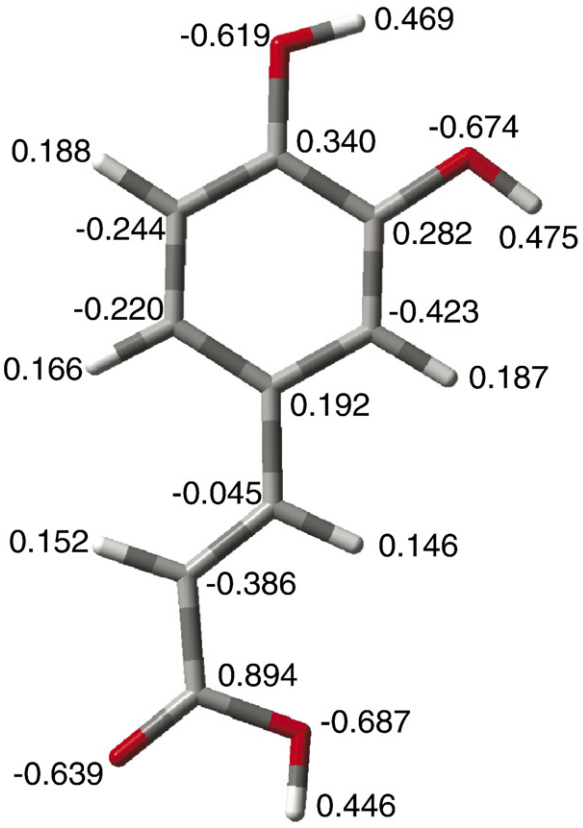

Fig. 10. Atomic charges of CA.

contrast to the other oxygen atoms, which exhibits negative charge values of −0.674, −0.639 and −0.619. Therefore, the carbon atom in the carboxylic acid group displays the highest positive charge (0.894). The carbon atoms in the aromatic ring are negatively charged. Nevertheless, in the aromatic ring with electron-withdrawing groups, the carbon atoms, which are connected to these kinds of groups, are positively charged.

4. Conclusions

The properties of the SWCNT:graphite-based electrode have been demonstrated. The SWCNT:graphite-based electrode offers a diametric improvement in the electrochemical behavior of caffeic acid. A pair of well-defined redox waves was obtained. The CA electrochemical behavior at the SWCNT:graphite-based electrode was controlled by adsorption and the electrode process on the surface of the graphite-based electrode was a diffusion-controlled process, involving two-charges accompanied by a transfer of two protons. The SWCNT:graphite-based electrode displayed promising promotion of the CA electrochemical reaction. The attractive properties of this new composite material open a new entrance for new electrodes in the field of electrochemical applications.

Acknowledgements

The authors would like to thank Mr. Hashemi for the performance of the SEM and TEM studies from the Science College Electron Microscopy Laboratory, University of Tehran. Moreover, the financial support provided by the Research Affairs of the University of Tehran is gratefully acknowledged.

References

[1] S. Iijima, Helical microtubes of graphitic carbon, Nature 354 (1991) 56–58.
[2] P.G. Wiles, J. Abrahamson, Carbon fibre layers on arc electrodes—I their properties and cool-down behavior, Carbon 16 (1978) 341–349.
[3] J. Abrahamson, P.G. Wiles, B.L. Rhoades, Structure of carbon fibres on carbon arc anodes, Carbon 37 (1999) 1873–1874.
[4] S. Iijima, T. Ichihashi, Single-shell carbon nanotubes of 1-nm diameter, Nature 363 (1993) 603–605.
[5] D.S. Bethune, C.H. Kiang, M.D. de Vries, G. Gorman, R. Savoy, J. Vazquez, R. Beyers, Cobalt-catalysed growth of carbon nanotubes with single-atomic-layer walls, Nature 363 (1993) 605–607.
[6] T.W. Odom, J.L. Huang, P. Kim, C.M. Lieber, Atomic structure and electronic properties of single-walled carbon nanotubes, Nature 391 (1998) 62–64.
[7] D. Tekleab, R. Czerw, D.L. Carroll, P.M. Ajayan, Electronic structure of kinked multiwalled carbon nanotubes, Appl. Phys. Lett. 76 (2000) 3594–3596.
[8] J.M. Nugent, K.S.V. Santhanam, A. Rubio, P.M. Ajayan, Fast electron transfer kinetics on multiwalled carbon nanotube microbundle electrodes, Nano Lett. 1 (2001) 87–91.
[9] F. Kurusu, H. Tsunoda, A. Saito, A. Tomita, A. Kadota, N. Kayahara, I. Karube, M. Gotoh, The advantage of using carbon nanotubes compared with edge plane pyrolytic graphite as an electrode material for oxidase-based biosensors, Analyst 131 (2006) 1292–1298.
[10] J. Wang, M. Musameh, Y. Lin, Solubilization of carbon nanotubes by Nafion toward the preparation of amperometric biosensors, J. Am. Chem. Soc. 125 (2003) 2408–2409.
[11] J. Wang, M. Musameh, Carbon nanotube/teflon composite electrochemical sensors and biosensors, Anal. Chem. 75 (2003) 2075–2079.
[12] A. Baghestani, C. Lemieux, G.D. Leroux, R. Baziramkenga, R.R. Simard, Determination of allelochemicars in spring cereal cultivars of different competitiveness, Weed Sci. 47 (1999) 498–504.
[13] M. Singh, R.V. Tamma, H.N. Nigg, HPLC identification of allelopathic compounds from lantana-camara, J. Chem. Ecol. 15 (1989) 81–89.
[14] R.M. Bostock, S.M. Wilcox, G. Wand, Suppression of *Monilinia fructicola* cutinase production by peach fruit surface phenolic acids, Physiol. Mol. Plant Pathol. 54 (1999) 37–50.
[15] F. Chinnici, A. Bendini, A. Gaiani, C. Riponi, Radical scavenging activatives of peels and pulps from cv. Golden delicious apples as related to their phenolic composition, J. Agric. Food Chem. 52 (2004) 4684–4689.
[16] H. Ravn, C. Andary, G. Kovacs, P. Molgaard, Caffeic acid–esters as invitro inhibitors of plant pathogenic bacteria and fungi, Biochem. Syst. Ecol. 17 (1989) 175–184.
[17] B.L. Bowles, A.J. Miller, Caffeic acid activity against clostridium–botulinum spores, J. Food Sci. 59 (1994) 905–908.
[18] R.D. Reinders, S. Biesterveld, P.J.H. Bijker, Survival of *Escherichia coli* O157: H7 ATCC 43895 in a model apple juice medium with different concentrations of proline and caffeic acid, Appl. Envirol. Microbiol. 67 (2001) 2863–2866.
[19] C.B. Summers, G.W. Folten, Prooxidant effects of phenolic-acids on the generalist herbivore helicoverpa-zea (Lepidoptera, noctuidae)—potential mode of action for phenolic-compounds in plant anti-herbivore chemistry, Insect Biochem. Mol. Biol. 24 (1994) 943–953.
[20] M. Cvikrova, J. Nedelnik, J. Eder, P. Binarova, Changes in pattern of phenolic-acids induced by culture filtrate of fusarium–oxysporum in alfalfa plants differing in susceptibility to the pathogen, J. Plant Physiol. 142 (1993) 1–5.
[21] E.A. Maher, N.J. Bate, W. Ni, Y. Elkind, R.A. Dixon, C.J. Lamb, Increased disease susceptibility of transgenic tobacco plants with suppressed levels of preformed phenylpropanoid products, Proc. Natl. Acad. Sci. U. S. A. 91 (1994) 7802–7806.
[22] M.E. Snook, E.S. Data, S.J. Kays, Characterization and quantitation of hexadecyl, octadecyl, and eicosyl esters of *p*-coumaric acid in the vine and

root latex of sweet-potato [impomoea-batatas (l) lam], J. Agric. Food Chem. 42 (1994) 2589–2595.
[23] C.B. Faulds, G. Williamson, The role of hydroxycinnamates in the plant cell wall, J. Sci. Food Agric. 79 (1999) 393–395.
[24] J. Friend, Phenolic substances and plant disease, Annu. Proc. Phytochem. Soc. 25 (1985) 367–392.
[25] T. Nagaoka, A.H. Banskota, Y. Tezuka, I. Saiki, S. Kadota, Selective antiproliferative activity of caffeic acid phenethyl ester analogues on highly liver-metastatic murine colon 26-L5 carcinoma cell line, Bioorg. Med. Chem. 10 (2002) 3351–3359.
[26] A. Bayandori Moghaddam, F. Kobarfard, A.R. Fakhari, D. Nematollahi, S.S. Hosseiny Davarani, Mechanistic study of electrochemical oxidation of o-dihydroxybenzenes in the presence of 4-hydroxy-1-methyl-2(1H)-quinolone — application to the electrochemical synthesis, Electrochim. Acta 51 (2005) 739–744.
[27] A. Bayandori Moghaddam, M.R. Ganjali, P. Norouzi, M. Niasari, A green method on the electro-organic synthesis of new caffeic acid derivatives: electrochemical properties and LC-ESI-MS analysis of products, J. Electroanal. Chem. 601 (2007) 205–210.
[28] J.N. Ke, S.-S. Lu, S.-H. Cheng, A strategy for the determination of dopamine at a bare glassy carbon electrode: *p*-phenylenediamine as a nucleophile, Electrochem. Commun. 8 (2006) 1514–1520.
[29] Y.-H. Bi, Z.-L. Huang, Y.-D. Zhao, Interactions of cytochrome *c* with DNA at glassy carbon surface, Biophys. Chem. 116 (2005) 193–198.
[30] S. Kallel Trabelsi, N. Belhadj Tahar, R. Abdelhedi, Electrochemical behavior of caffeic acid, Electrochim. Acta 49 (2004) 1647–1654.
[31] A. Bayandori Moghaddam, M.R. Ganjali, P. Norouzi, M. Latifi, A green method for the electroorganic synthesis of new 1,3-indandione derivatives, Chem. Pharm. Bull. 54 (2006) 1391–1396.
[32] S. Suzen, B.T. Dermircigil, S.A. Ozkan, S. Suzen, B.T. Dermircigil, S.A. Ozkan, Electroanalytical evaluation and determination of 5-(3-indolyl)-2-thiohydantoin derivatives by voltammetric studies: possible relevance to in vitro metabolism, New J. Chem. 6 (2003) 1007–1011.
[33] M.J. Frisch, G.W. Trucks, H.B. Schlegel, G.E. Scuseria, M.A. Robb, J.R. Cheeseman, V.G. Zakrzewski, J.A. Montgomery Jr., R.E. Stratmann, J.C. Burant, S. Dapprich, J.M. Millam, A.D. Daniels, K.N. Kudin, M.C. Strain, O. Farkas, J. Tomasi, V. Barone, M. Cossi, R. Cammi, B. Mennucci, C. Pomelli, C. Adamo, S. Clifford, J. Ochterski, G.A. Petersson, P.Y. Ayala, Q. Cui, K. Morokuma, D.K. Malick, A.D. Rabuck, K. Raghavachari, J.B. Foresman, J. Cioslowski, J.V. Ortiz, A.G. Baboul, B.B. Stefanov, G. Liu, A. Liashenko, P. Piskorz, I. Komaromi, R. Gomperts, R.L. Martin, D.J. Fox, T. Keith, M.A. Al-Laham, C.Y. Peng, A. Nanayakkara, C. Gonzalez, M. Challacombe, P.M.W. Gill, B. Johnson, W. Chen, M.W. Wong, J.L. Andres, C. Gonzalez, M. Head-Gordon, E.S. Replogle, J.A. Pople, GAUSSIAN 98, Revision A.7, Gaussian, Inc., Pittsburgh, PA, 1998.
[34] P.J. Britto, K.S.V. Santhanam, A. Rubio, J.A. Alonso, P.M. Ajayan, Improved charge transfer of carbon nanotube electrodes, Adv. Mater. 11 (1999) 154–157.
[35] R.S. Nicholson, I. Shain, Theory of stationary electrode polarography: single scan and cyclic methods applied to reversible, irreversible and kinetic systems, Anal. Chem. 36 (1964) 706–723.
[36] A.J. Bard, L.R. Faulkner, Electrochemical Methods: Fundamentals and Applications, 2nd ed., John Wiley & Sons, New York, 2001.
[37] M. Namazian, H.R. Zare, Computational electrode potential of a coumestan derivative: theoretical and experimental studies, Biophys. Chem. 117 (2005) 13–17.